AGU100 ADVANCING EARTH AND SPACE SCIENCE

Water Resources Research

RESEARCH ARTICLE
10.1029/2018WR022816

Climate Elasticity of Low Flows in the Maritime Western U.S. Mountains

M. G. Cooper[1], J. R. Schaperow[2], S. W. Cooley[1,3], S. Alam[2], L. C. Smith[1], and D. P. Lettenmaier[1]

[1]Department of Geography, University of California, Los Angeles, CA, USA, [2]Department of Civil and Environmental Engineering, University of California, Los Angeles, CA, USA, [3]Institute at Brown for the Environment and Society, Brown University, Providence, RI, USA

Key Points:
- Summer low-flow elasticity to evaporative demand is larger than elasticity to winter precipitation in every catchment studied in the maritime western United States
- Summer low-flow elasticity to evaporative demand and winter precipitation is smaller in snow-dominated catchments, on average
- Summer low-flow elasticity to evaporative demand and winter precipitation is smaller in slow-draining catchments, on average

Supporting Information:
- Supporting Information S1
- Table S1

Correspondence to:
D. P. Lettenmaier,
dlettenm@ucla.edu

Citation:
Cooper, M. G., Schaperow, J. R., Cooley, S. W., Alam, S., Smith, L. C., & Lettenmaier, D. P. (2018). Climate elasticity of low flows in the maritime western U.S. mountains. *Water Resources Research*, *54*, 5602–5619. https://doi.org/10.1029/2018WR022816

Received 20 FEB 2018
Accepted 8 JUL 2018
Accepted article online 21 JUL 2018
Published online 19 AUG 2018
Corrected 27 AUG 2019

This article was corrected on 27 AUG 2019. See the end of the full text for details.

Abstract Summer streamflow is an important water resource during the dry summers in the western United States, but the sensitivity of summer minimum streamflow (low flow) to antecedent winter precipitation as compared with summer evaporative demand has not been quantified for the region. We estimate climatic elasticity of low flow (percent change in low flow divided by percent change in climatic forcing variable) with respect to annual maximum snow water equivalent (E_{SWE}), winter precipitation (E_{PPT}), and summer potential evapotranspiration (E_{PET}) for 110 unmanaged headwater catchments in the maritime western U.S. mountains. We find that $|E_{PET}|$ is larger than $|E_{PPT}|$ and $|E_{SWE}|$ in every catchment studied and is 4–5 times larger than both, on average. Spatial variations in E are dominated by three patterns. First, $|E_{PPT}|$, $|E_{SWE}|$, and $|E_{PET}|$ are largest and most variable among semiarid catchments and decrease nonlinearly with increasing values of the humidity index (the ratio of annual precipitation to annual evaporative demand). Second, $|E_{PPT}|$ and $|E_{PET}|$ are lower in snow-dominated catchments than in rain-dominated catchments, suggesting that snow cover reduces the proportional response of low flows to climatic variability. Third, $|E_{PPT}|$, $|E_{SWE}|$, and $|E_{PET}|$ are lower in slow-draining catchments than in fast-draining catchments, for which baseflow recession storage coefficients are used to represent the rate at which catchment water storage is translated into streamflow. Our results provide the first comparison of summer low-flow elasticity to PPT versus PET and its spatial variation in the maritime western U.S. mountains.

Plain Language Summary The western U.S. climate is characterized by cool, wet winters and warm, dry summers. Streamflow provides a critical water resource during the dry summers here. The minimum streamflow (low flow) usually occurs in September or October, several months after the mountain snowpack has melted. The magnitude of the low flow sets a lower bound on water supply, especially in systems without surface water storage. However, it is not clear whether the magnitude of the low flow is more strongly controlled by how cold and wet the previous winter was versus how warm and dry the summer was. We quantified the percent change in low flows per 1% change in winter precipitation and summer evaporative demand. We found that percent changes in low flows are 4 to 5 times larger per 1% change in summer evaporative demand than winter precipitation. However, year-to-year variation in evaporative demand is small so the year-to-year variation in low flows is more strongly associated with year-to-year variation in winter precipitation. Our results suggest that low flows are highly vulnerable to small changes in evaporative demand, but more work is needed to understand expected changes in evaporation in a warming climate.

1. Introduction

Summer streamflow provides water for irrigated agriculture, power generation, municipal and industrial water supply, in-stream ecological habitat, and many other important societal and ecological needs during the dry Mediterranean summers in the maritime western United States (Arismendi et al., 2013; Hamlet et al., 2002; Jaeger et al., 2017; Mantua et al., 2010). The annual minimum streamflow (hereafter, low flow) usually occurs during late summer (September to October) here, following cessation of the spring snowmelt and summer streamflow recession (Kormos et al., 2016). Notwithstanding changes in catchment water storage, the annual streamflow magnitude reflects a balance between the annual precipitation supply and the evaporative energy demand (Milly, 1994), which in the maritime western United States are concentrated during winter and summer, respectively. However, the relative control of antecedent winter precipitation supply versus summer evaporative energy demand on summer low flows appears not to have been previously quantified for the region.

Interannual climate variability in the region is characterized by multiyear periods of below-average precipitation and persistent hydrologic drought (Dettinger, 2013; Van Loon, 2015). Economic consequences of drought are often severe here, especially when exacerbated by above-average air temperatures that reduce winter snow accumulation and, consequently, late summer water supply for irrigation and other economic activity (Howitt et al., 2015; Jaeger et al., 2017; Shukla et al., 2015). Moreover, the magnitude of the annual and summer low flow has declined since at least the middle twentieth century at nearly every unimpaired headwater stream gage in the Pacific Northwest and the Sierra Nevada mountains of California, coincident with a period of declining low- and middle-elevation mountain snowpack and annual precipitation (Jung et al., 2013; Kormos et al., 2016; Lins & Slack, 1999; Luce et al., 2013; Mote et al., 2018; Rice et al., 2015). Continued declines in mountain snowpack are expected as the regional air temperature continues to warm, whereas the magnitude and direction of expected precipitation changes are uncertain owing in part to the wide spread in future precipitation predicted by global and regional climate models (Gergel et al., 2017). Understanding the sensitivity of summer streamflow to different sources of climatic variability is therefore important, both for interpreting natural streamflow variations and for anticipating water scarcity in a changing climate.

Streamflow elasticity is one metric to quantify the climatic sensitivity of streamflow (Dooge, 1992; Schaake, 1990). Streamflow elasticity is defined as the fractional change in streamflow for a fractional change in a proximate forcing variable, for example, precipitation:

$$E(P,Q) = \frac{\mathrm{d}Q/Q}{\mathrm{d}P/P} = \frac{\mathrm{d}Q}{\mathrm{d}P}\frac{P}{Q} \tag{1}$$

where P and Q are precipitation and streamflow, respectively, and E is usually expressed as a percent change in Q per 1% change in P. Streamflow elasticity can be estimated empirically from historical time series of natural variations in P and Q (e.g., Sankarasubramanian et al., 2001) or by applying a synthetic dP and simulating dQ with a process-based hydrologic model (e.g., Vano et al., 2012).

Previous studies of streamflow elasticity to climate have generally focused on the elasticity of streamflow to precipitation as compared with air temperature (Milly et al., 2018). For the maritime western U.S. region, the magnitude of both annual streamflow (Jeton et al., 1996; Risbey & Entekhabi, 1996) and summer low flow (Kormos et al., 2016) appears to be more sensitive to precipitation magnitude than to air temperature. Air temperature has been invoked as a proxy for snowmelt timing and for its physical connection to evapotranspiration (Jeton et al., 1996; Kormos et al., 2016; Milly et al., 2018; Risbey & Entekhabi, 1996). Potential evapotranspiration is more directly related to the annual water balance than air temperature (Milly et al., 2018), but to our knowledge streamflow elasticity to potential evapotranspiration has not been quantified at the western U.S. regional scale for either annual or summer low flows. Consequently, the relative sensitivity of summer low flows to antecedent winter precipitation magnitude (moisture supply) versus summer potential evapotranspiration (moisture demand) is unknown.

Understanding spatial variations in streamflow sensitivity to climate is important for anticipating water scarcity at the local scale, especially in the diverse climatic and physiographic landscape of the western United States (Safeeq et al., 2014; Tague & Dugger, 2010). Three factors have been identified as important mediators of spatial variability of both annual and summer streamflow sensitivity to climate elsewhere or separately: (1) the humidity index P/PET, which reflects the degree to which the mean annual catchment water balance is energy limited ($P/PET > 1$) versus water limited ($P/PET < 1$); (2) the degree to which seasonal moisture supply is in phase with seasonal energy demand, for which the fraction of annual precipitation that falls as snow versus rain and/or the timing of snowmelt may be proxies; and (3) differences in the capacity of catchments to store water, and the rate at which catchment water storage is translated into streamflow (i.e. catchment-scale streamflow recession rates, hereafter drainage rates hereafter *drainage rates*), which reflects physiographic factors such as soil and rock porosity and permeability as well as catchment size, shape, and slope (Berghuijs et al., 2014; Harman et al., 2011; Milly, 1994; Sankarasubramanian et al., 2001; Tague & Grant, 2009; Wolock & McCabe, 1999). Differences in vegetation and land use/land cover change are also identified as important mediators of streamflow elasticity but are not examined here.

In the context of annual streamflow elasticity, water-limited (i.e., arid and semiarid) catchments are more sensitive to climatic variability than energy-limited (i.e., humid) catchments (Berghuijs et al., 2017). In addition, catchments where seasonal moisture supply is in phase with seasonal energy demand, or where

rainfall is a larger portion of annual precipitation than snowfall, are generally more sensitive to climatic variability (Milly, 1994; Sankarasubramanian et al., 2001). Drainage rates are known to mediate the climatic sensitivity of summer streamflow in the western United States (Safeeq et al., 2013, 2014; Tague & Grant, 2009), but to our knowledge the relationship between drainage rates and summer streamflow elasticity has not been quantified (other definitions of sensitivity were used). In most cases, these factors have been examined in the context of case studies, often hydrologic model based, or for a small number of catchments (e.g., Godsey et al., 2014; Harman et al., 2011; Jefferson et al., 2008; Markovich et al., 2016; Tague & Grant, 2009), with some exceptions (e.g., Safeeq et al., 2013). To our knowledge no study has examined how each of the three aforementioned factors mediate summer low-flow elasticity at the western U.S. regional scale. Consequently, the relative influence of these factors on spatial variations in summer low-flow elasticity is not currently known. Such understanding should provide useful context for case studies and process-based experiments, as well as provide water managers and scientists with a consistent and comprehensive view of summer low-flow elasticity to climate variability across the heterogeneous landscape of the maritime western United States.

Our goal here is to estimate the sensitivity of summer low-flow magnitude to variability in winter precipitation versus summer evaporative demand in maritime western U.S. mountain catchments. The two research questions that we address are (1) what is the sensitivity of summer minimum streamflow magnitude to annual maximum snow water equivalent (SWE_{MAX}), cumulative winter precipitation, and cumulative summer evaporative demand? and (2) how do climatic factors such as the humidity index (P/PET) and the ratio of SWE_{MAX} to annual precipitation (SWE/P) compare to drainage rates as mediators of spatial differences in these elasticities? We estimate summer low-flow elasticities for 110 unmanaged headwater catchments across a maritime latitudinal transect of the coastal western United States and show how they vary with latitude, P/PET, and SWE/P. Then we compare summer low-flow elasticities to baseflow recession storage coefficients, which we use as proxies for drainage rates or the rate at which seasonal changes in catchment water storage are translated into streamflow. To clarify the relative influence of the SWE/P ratio versus drainage rates on summer low-flow elasticities, we categorize catchments into rain- versus snow-dominated precipitation regimes and fast- versus slow-draining hydrologic regimes (Figure 1). Finally, we discuss the implications of our findings for anticipating the response of summer streamflow to climate change in the maritime western United States.

2. Study Area and Data

We restricted our analysis to catchments located in the maritime mountain ranges of California, Oregon, and Washington states, United States (Figure 2). The study catchments span a range of climatic conditions, from the semiarid California coastal mountains and southern Sierra Nevada to the humid, snow-dominated Cascades in northern Washington. More than two thirds of the annual precipitation in the region occurs during winter (which we define as November–March), although the ratio of cumulative winter precipitation to cumulative annual precipitation decreases markedly from south to north (Figure 2).

2.1. Streamflow Data

We selected candidate streamflow gages from the U.S. Geological Survey's (USGS's) Geospatial Attributes of Gages for Evaluating Streamflow, version II (GAGES-II) reference database (Falcone, 2011; Falcone et al., 2010). Reference gages are considered to be relatively unimpaired by anthropogenic activity and suitable for studies of natural streamflow variability and change. We obtained daily streamflow data for all reference gages from the USGS Surface-Water Data for the Nation online database (waterdata.usgs.gov/nwis/sw). We restricted our analysis to the 1948–2015 time period and excluded gages with $<$30 years of data during this period. To check the influence of missing values, we repeated our analysis using gages with maximum 10 years missing data and found no material difference in results; therefore, we retained the 30-year threshold to maintain a robust sample size and for consistency with earlier studies (Fritze et al., 2011; Safeeq et al., 2013; Stewart et al., 2005). We excluded gages with remarks in the USGS Annual Water Data Report (wdr.water.usgs.gov) noting flow regulation or upstream water diversions that may alter low flows due to factors unrelated to natural climate variability. We then plotted each record of daily streamflow and excluded gages with evidence of step shifts, discontinuities, unrealistic constant flow values, and outliers on log flow versus time plots, with particular attention to low-flow periods. We excluded one catchment with glacial headwaters

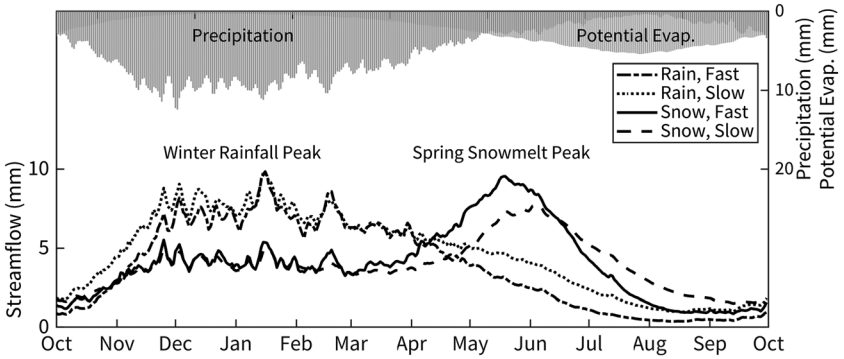

Figure 1. Ensemble mean hydrographs of basin mean daily streamflow for all catchments in four different hydroclimatic categories that demonstrate the range of hydrograph characteristics in the study region: rain-dominated catchments that are also slow draining (rain, slow), rain-dominated catchments that are also fast draining (rain, fast), snow-dominated catchments that are also slow draining (snow, slow), and snow-dominated catchments that are also fast draining (snow, fast; adapted from Safeeq et al., 2013). Top axis shows mean annual precipitation and potential evapotranspiration concentrated during winter and summer, respectively, averaged across all study catchments.

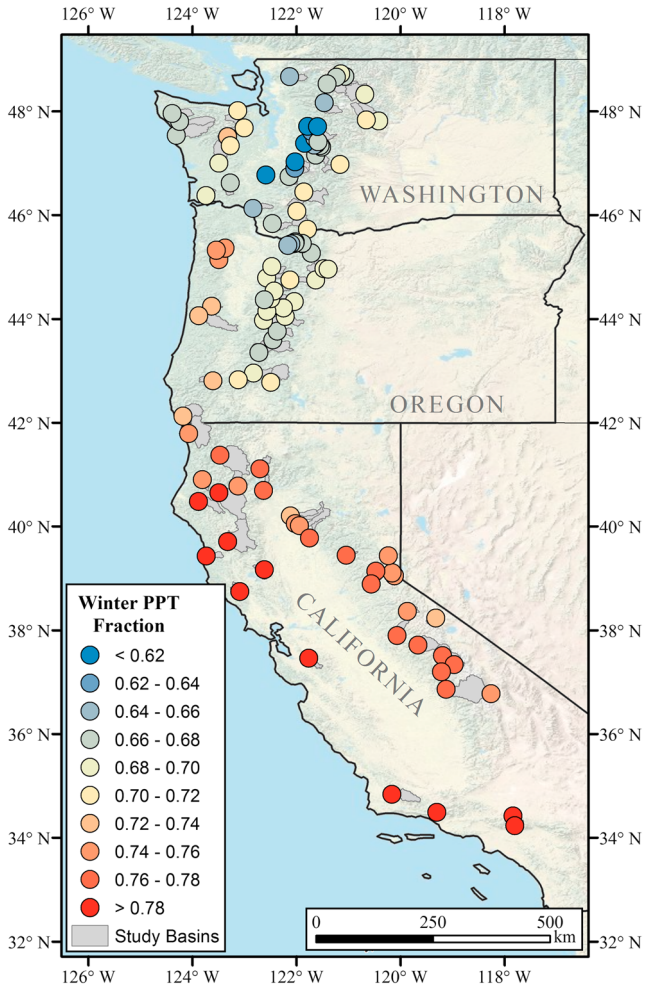

Figure 2. The study catchments and their ratio of cumulative winter (November to March) precipitation to cumulative annual precipitation (P_W/P).

(station 12182500) that passed screening to avoid the influence of glacier melt on its low flows. Our screening process resulted in the 110 gages shown in Figure 2 (also see the supporting information).

Following Godsey et al. (2014), we defined the summer minimum streamflow (Q_{MIN}) as the minimum of the 15-day running median streamflow between 1 June and 31 October of each calendar year. We chose this period to avoid detecting annual minimum flows that occasionally occur during cold dry periods between November and May in our study area (Kormos et al., 2016). To this end, Q_{MIN} is representative of the summer dry season, which in our study area extends through October prior to onset of winter rains in November (Kormos et al., 2016). The time series of Q_{MIN} for each gage that resulted from this process formed the basis for our subsequent analysis.

2.2. Climate Data and Related Metrics

We extracted gridded fields of daily precipitation, SWE, and climatic variables needed to compute Penman-Monteith reference crop evapotranspiration for each catchment from the Livneh et al. (2015) 1/16° data set. The Livneh et al. (2015) gridded precipitation data were interpolated from point observations at National Climatic Data Center Cooperative Observer stations and scaled to match the Parameter-Elevation Regressions on Independent Slopes Model 1981–2010 precipitation climatology. The gridded SWE fields are model output from the variable infiltration capacity hydrologic model forced with other fields (including precipitation and air temperature) in the Livneh et al. (2015) data set. The variable infiltration capacity model (Liang et al., 1994) simulates the land-surface energy balance and water balance at 1/16° horizontal grid spacing and 3-hourly time step (aggregated to daily) and has been used in previous analyses within our study area (e.g., Mao et al., 2015; Mote et al., 2018). We computed reference evapotranspiration as a surrogate for potential evapotranspiration following Allen et al. (1998). Variables needed to compute reference evapotranspiration include 2-m surface air temperature, net radiation, vapor pressure deficit, and wind speed. The reference *crop* was short grass with a prescribed surface resistance of 70 s/m (Allen et al., 1998).

To improve sampling resolution near catchment edges, we resampled the 1/16° gridded data to 1/160° using bilinear interpolation. We computed catchment mean area-weighted daily records of precipitation, SWE, and potential evapotranspiration from the resampled data, from which we computed annual time series of cumulative 1 November to 31 March (winter) precipitation (*PPT*), annual maximum SWE (SWE_{MAX}), and cumulative 1 June to 30 September (summer) potential evapotranspiration (*PET*). We used these records to compute the ratio of cumulative annual precipitation to cumulative annual potential evapotranspiration, that is, the *humidity index* (*P*/*PET*; Budyko, 1974) and the ratio of annual maximum SWE to cumulative annual precipitation (*SWE*/*P*). These metrics were computed for each catchment and each water year and then averaged across all years to produce one representative value for each catchment.

3. Methods

3.1. Elasticity Analysis

We estimated Q_{MIN} sensitivity to SWE_{MAX}, *PPT*, and *PET* using elasticity analysis (Schaake, 1990). Streamflow elasticity is the fractional change in streamflow for a given fractional change in precipitation or similar climate metric. Streamflow elasticity can be estimated from empirical relationships between historical streamflow and climate observations (for which Sankarasubramanian et al., 2001, describe several estimators) and from process-based hydrologic model simulations (as in Vano et al., 2012). Both methods have advantages and disadvantages. For example, interannual carryover (persistence) is usually ignored in statistical models, whereas model structural error is an issue for hydrologic models. Here we used observation-based estimators to avoid hydrologic model error.

We estimated Q_{MIN} elasticity using ordinary least squares log-log linear regression between annual time series of Q_{MIN} and SWE_{MAX}, *PPT*, and *PET* (Jenicek et al., 2016). The method is equivalent to the bivariate parametric estimator described by Sankarasubramanian et al. (2001). We computed elasticity (*E*) as the inverse transformed regression slope as follows:

$$E = 1 - \exp(a*\beta), \tag{2}$$

where $a = \log(1 + \Delta)$, $\Delta = 1\%$, and β is the regression slope. Setting $\Delta = 1\%$ means *E* is interpreted as the percent change in Q_{MIN} per 1% change in SWE_{MAX}, *PPT*, and *PET*. We refer hereafter to these elasticities as E_{SWE}, E_{PPT}, and E_{PET}. For ordinary least squares regression, the slope is

$$\beta = r_{X,Y}\frac{S_Y}{S_X}, \tag{3}$$

where $r_{X,Y}$ is the Pearson correlation coefficient for independent variable *X* and dependent variable *Y*, and S_Y and S_X are the sample standard deviations. Equation (3) says that the slope of a linear regression β is proportional to the correlation between two variables scaled by the ratio of their standard deviations (here interannual climate variability). Previous studies have used β as a direct estimate of *E* (e.g., Godsey et al., 2014). Owing to our use of log-log regression, we estimated *E* with equation (2), but for the range of $a * \beta$ values considered in this study, $E \sim \beta$ and hence $E \sim r_{X,Y}\frac{S_Y}{S_X}$.

We used equation (3) to determine the relative influence of $r_{X,Y}$ and S_Y/S_X on *E*. This is important when interpreting differences between E_{SWE}, E_{PPT}, and E_{PET} or between categories of catchments within the E_{SWE}, E_{PPT}, and E_{PET} populations. For example, we categorize catchments based on precipitation regime (rain dominated versus snow dominated), as described in section 3.3. Differences in *E* between these categories are related to differences in $r_{X,Y}$ and S_Y/S_X that are not evident from *E* alone. Similarly, we show that *PET* has very small interannual variability compared to *PPT* and Q_{MIN} (i.e., $S_{PET} \ll S_{PPT}$). It follows that for similar $|r|$, $S_{Q_{MIN}}/S_{PET} \gg S_{Q_{MIN}}/S_{PPT}$ and thus $|E_{PET}| \gg |E_{PPT}|$. While this result is expected, it demonstrates that the magnitude of $|E|$ is highly sensitive to the magnitude of historic variability in the independent climatic variable of interest (e.g., *PET* versus *PPT*). Therefore, the magnitude of expected future change in the independent variable must be considered when interpreting *E* in terms of vulnerability to climate change.

Prior work has shown poor goodness of fit can lead to unreliable elasticity estimates (Tsai, 2017). Because one goal of this study is to infer the influence of physical processes on spatial variations in *E*, we exclude elasticities with *p* values >0.05 to avoid biasing these interpretations. Where applicable, we report ensemble mean

and median values for the entire set of 110 study catchments along with ensemble mean and median values for the set of statistically significant elasticities. We used the False Discovery Rate method (Khaliq et al., 2009) to assess field significance of the elasticity regressions at 95% confidence, which detects the discovery of statistically significant correlation at the individual site (i.e., local) significance level by chance alone.

3.2. Baseflow Recession Analysis

We used baseflow recession storage coefficients as proxies for drainage rates, or the rate at which seasonal changes in catchment water storage are translated into streamflow (Safeeq et al., 2013, 2014; Tague & Grant, 2009). We used baseflow recession analysis (Tallaksen, 1995) to estimate the storage-discharge relationship for each stream gage record:

$$Q = kS^b, \tag{4}$$

where Q is the rate of streamflow out of the catchment [L T^{-1}], S is storage in catchment aquifers [L], k is the characteristic time scale of the baseflow recession process [L^{1-b} T^{b-2}], and b is a dimensionless constant. For baseflow conditions where recharge (e.g., precipitation or snowmelt) to the catchment aquifers is negligible, $dS/dt = -Q$ and hence

$$-\frac{dQ}{dt} = kQ^b. \tag{5}$$

Representing the baseflow recession process in the form of equation (5) is advantageous because the linearized solution ($b = 1$) to the Boussinesq equation for drainage of an unconfined horizontal aquifer can be expressed in the same form, where the coefficient k is a function of the aquifer hydraulic conductivity, porosity, and geometry (Brutsaert & Nieber, 1977). Hence, k reflects the intrinsic geologically mediated hydraulic properties of the upstream catchment aquifers. The inverse $1/k$ is the characteristic e-folding time scale [T for $b = 1$] of the baseflow recession process and is commonly referred to as the storage coefficient (Brutsaert, 2008, 2010). Storage coefficients (hereafter K) can be used to estimate changes in groundwater storage from Q (Brutsaert, 2008, 2010) or, as in this study, to infer the extent to which Q is influenced by seasonal changes in groundwater storage (Tague & Grant, 2004).

We estimated K for each catchment using the dQ/dt versus Q method (Brutsaert & Nieber, 1977). The method consists of plotting $|dQ/dt|$ versus Q on log-log scale and fitting a least squares solution with slope $b = 1$ and intercept k (equation (5) in log-space) to the lower fifth percentile of values. The lower fifth percentile is selected under the assumption that these values represent the best estimate of baseflow, that is, flow not influenced by external inputs and representative of aquifer contributions to streamflow (Brutsaert & Nieber, 1977). Prior to fitting, we removed all Q on days with precipitation >0 and for 3 days following, all Q on days with $dQ/dt > 0$, and all Q between the date of SWE_{MAX} and 15 August (as in Brutsaert & Nieber, 1977; Safeeq et al., 2013). The latter criterion was used to remove the influence of snowmelt recharge. We apply a variable dt to account for artifacts associated with the precision of the discharge measurements following Rupp and Selker (2006a) and Sánchez-Murillo et al. (2015).

We acknowledge that the linear assumption ($b = 1$) is problematic where slope is an important driver of flow (Rupp & Selker, 2006b), such as the montane catchments analyzed here. Empirical studies also suggest that b varies spatially with catchment climatic or physiographic characteristics (Berghuijs et al., 2016; Ye et al., 2014). However, for our purposes, K is used to indicate whether the baseflow recession process is weakly versus strongly controlled by seasonal changes in deep groundwater storage versus shallow subsurface flow (Safeeq et al., 2013; Tague & Grant, 2004) and is not used to estimate hydraulic properties of the catchment aquifers.

3.3. Catchment Classifications

To summarize differences in E_{SWE}, E_{PPT}, and E_{PET} based on differences in seasonal snow accumulation versus drainage rates, we categorized the catchments into precipitation and hydrologic regimes. The precipitation regimes are rain dominated ($SWE/P < 20\%$) and snow dominated ($SWE/P \geq 20\%$). We tested different rain/snow threshold values including the mean and median of the SWE/P distribution of our study catchments and higher thresholds ($SWE/P \geq 30\%$). We found no material effect on our results other than to

skew the sample size toward the rain-dominated category; therefore, we selected 20% to broadly distinguish between rain- and snow-dominated catchments.

The hydrologic regimes are fast draining ($K < 45$ days) and slow draining ($K \geq 45$ days). We chose $K = 45$ days based on the global analysis of K values reported by Brutsaert (2008, 2010). As with the *SWE*/*P* threshold, our results are robust to different threshold K values including the mean and median of the K value distribution of our study catchments, which we show are nearly identical to those of Brutsaert (2008, 2010). We emphasize that *fast draining* and *slow draining* are heuristics meant to describe catchments where the baseflow recession process is weakly versus strongly controlled by seasonal changes in deep groundwater storage versus shallow subsurface flow processes (Safeeq et al., 2013; Tague & Grant, 2004, 2009). We used these catchment classifications to assess differences in E_{SWE}, E_{PPT}, and E_{PET} between these distinct climatic and hydrologic regimes. In addition to the categorical comparisons, we used the nonparametric Spearman rank correlation (ρ) to assess relationships between E values and K values, and between E values and *SWE*/*P* ratios.

4. Results

Our analysis is intended to determine the sensitivity of summer low flows to winter precipitation as contrasted with summer evaporative demand and how climatic versus hydrologic factors mediate these sensitivities. We first show the spatial structure of summer low-flow elasticity (E) across our maritime latitudinal transect and examine how E varies with (1) latitude and the humidity index, (2) snow accumulation and snowmelt timing, and (3) drainage rates.

4.1. Goodness of Fit

We find locally significant ($p \leq 0.05$) E_{SWE}, E_{PPT}, and E_{PET} values in 61, 69, and 93 of the 110 study catchments, respectively. Of these locally significant values, 61, 67, and 92 are field significant at 95% confidence. A chi-square test suggests that the E_{SWE} values are normally distributed; however, the E_{PPT} and E_{PET} distributions are positively and negatively skewed, respectively. The median E_{SWE}, E_{PPT}, and E_{PET} across the locally significant values are 0.30%, 0.50%, and −2.4%, respectively. When compared across all 110 study catchments (i.e., retaining E values without significant correlation), the median E_{SWE}, E_{PPT}, and E_{PET} are 0.16%, 0.35%, and −2.2%, respectively. In total, 49 catchments were classified as snow dominated (mean $SWE/P \geq 20\%$), of which we find 40, 40, and 41 with locally significant E_{SWE}, E_{PPT}, and E_{PET} values, respectively. When compared across these snow-dominated catchments, the median E_{SWE}, E_{PPT}, and E_{PET} are 0.43%, 0.50%, and −2.1%, respectively. Together, these median values suggest that Q_{MIN} is ~4–5 times more sensitive to *PET* than both *PPT* and *SWE*. Hereafter, we report results for the set of locally significant regressions.

The goodness of fit (R^2) ranges from 0.06 to 0.82 (Figure 3), with mean R^2 of 0.30, 0.33, and 0.30, respectively, suggesting that Q_{MIN} shares a nearly identical weighting of underlying causal factors with *SWE*, *PPT*, and *PET*, taken separately. This similarity in R^2 (and hence r) between variables suggests that, on average, differences between E_{SWE}, E_{PPT}, and E_{PET} are driven by differences in the ratio of interannual Q_{MIN} variability to climatic variability (i.e., S_Y/S_X, equation (2)). Catchments with the poorest goodness of fit tend to be those with the smallest $|E|$ values. For example, compare the R^2 and E values of the best fit regressions (Figures 3a–3c) to the worst fit regressions (Figures 3d–3f).

4.2. Latitudinal Variation in the Magnitude and Timing of Moisture Supply Versus Demand

Absolute E values are negatively correlated with latitude for catchments located south of ~40°N (near the border between California and Oregon; Figure 4). The largest $|E|$ values are found in the snow-dominated Sierra Nevada (~36–39°N) and rain-dominated coastal California catchments, and the smallest $|E|$ values in the Oregon and Washington Cascades and coastal catchments of the Pacific Northwest. We find a similar pattern of decreasing R^2 with increasing latitude for E_{SWE} and E_{PPT}, suggesting that correlation between Q_{MIN} and winter precipitation weakens with increasing latitude from California to the Pacific Northwest. Conversely, R^2 increases with latitude for E_{PET}, suggesting a stronger relationship between Q_{MIN} and summer evaporative demand in the Pacific Northwest.

The pattern of decreasing $|E|$ with increasing latitude corresponds with an increase in the humidity index *P*/*PET* with latitude in the study area (Figure 5). South of ~40°N in the Sierra Nevada and coastal California mountains, *P*/*PET* is close to or <1, indicating primarily water-limited conditions on annual time scales. In

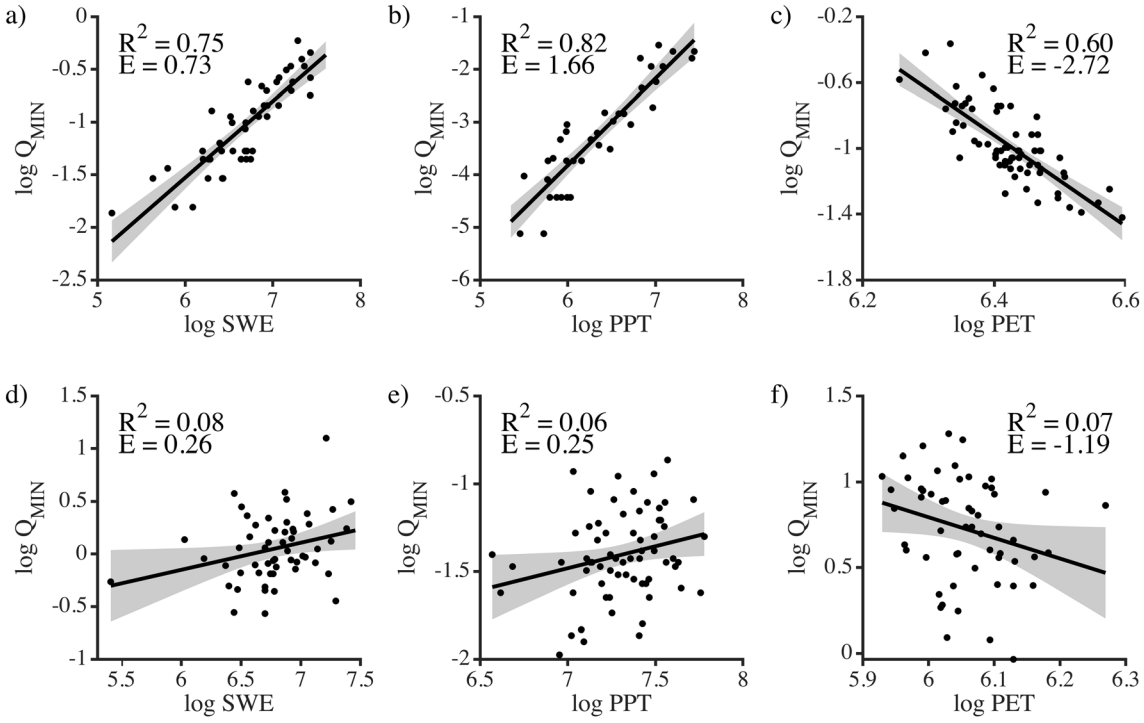

Figure 3. Examples of (a–c) best fit and (d–f) worst fit regressions for E_{SWE}, E_{PPT}, and E_{PET}. The R^2 and E value (%) are shown for each regression.

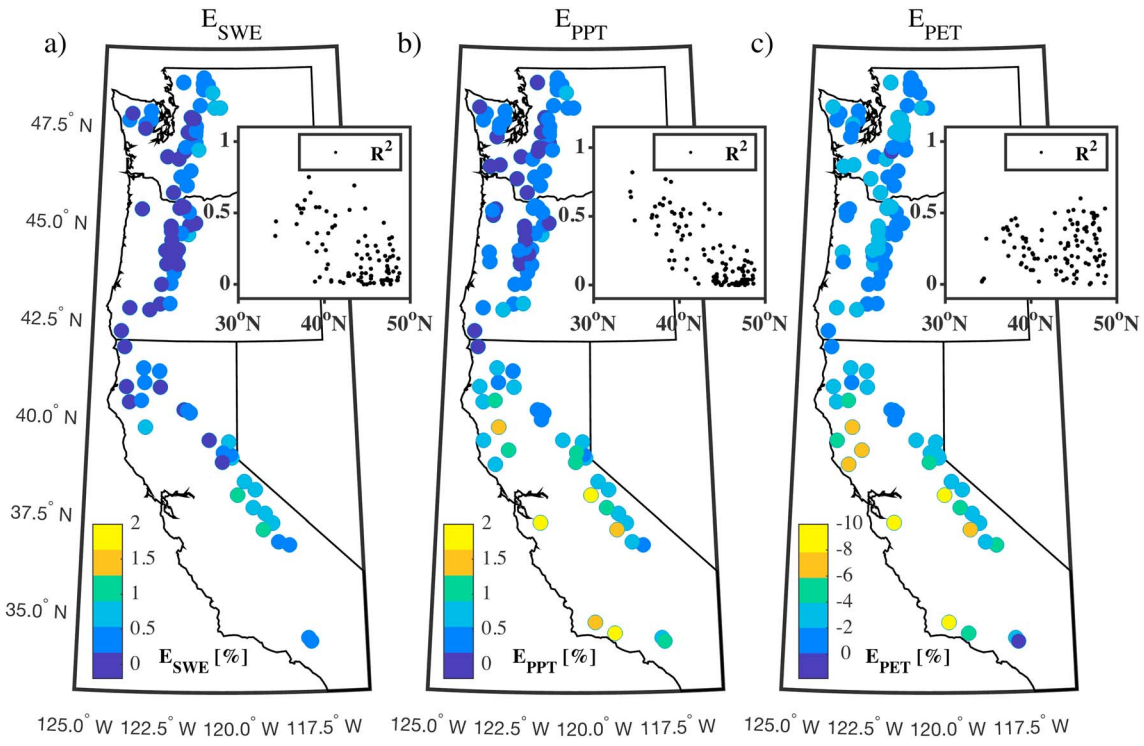

Figure 4. (a) E_{SWE}, (b) E_{PPT}, and (c) E_{PET} for the set of 110 study catchments (excluding those with mean annual $SWE/P < 5\%$ for E_{SWE}). Circles are color coded by the E value of each catchment. Insets show relationships between R^2 and latitude for the E_{SWE}, E_{PPT}, and E_{PET} regressions.

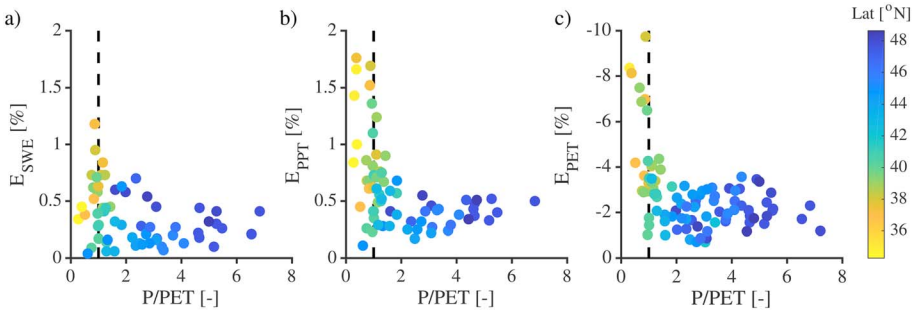

Figure 5. (a) E_{SWE}, (b) E_{PPT}, and (c) E_{PET} versus the humidity index *P/PET*, for catchments with locally significant ($p \leq 0.05$) elasticity regressions. Symbols are color coded by the latitude of the catchment centroids. The vertical dashed line at *P/PET* = 1 demarcates energy-limited conditions to the right of the dashed line from water-limited conditions to the left.

this region, small increases in moisture supply *P* relative to demand *PET* are associated with large decreases in $|E_{SWE}|$, $|E_{PPT}|$, and $|E_{PET}|$. North of ~40°N in the Cascades and coastal mountains of the Pacific Northwest, *P/PET* is generally >1, indicating primarily energy-limited conditions and an annual surplus of *P* relative to *PET*. $|E|$ values in this region are consistently lower, more homogeneous, and do not vary systematically with *P/PET*. In both regions, the increase in *P/PET* with latitude is driven by both an increase in *P* and a decrease in *PET* with latitude, but *P* increases at approximately twice the rate of decrease in *PET*. Mean annual *P* increases from ~500 to ~2,800 mm/year at the southern and northern ends of the transect, respectively, whereas mean annual *PET* decreases from ~1,400 to ~600 mm/year, respectively. Consequently, the variability in *E* with latitude shown in Figure 4 is associated with variability in *P* more than in *PET*.

In addition to indices of mean annual water supply and demand such as the humidity index, previous work has indicated enhanced climatic sensitivity of annual streamflow for catchments where seasonal moisture supply is in phase with seasonal energy demand (Milly, 1994; Sankarasubramanian et al., 2001). Given the seasonal nature of summer low flows, this leads to an expectation that summer low-flow elasticity depends on seasonal moisture supply and energy demand phasing. To quantify phasing, we compute the centers of timing of annual precipitation (CT_{PPT}) and potential evapotranspiration (CT_{PET}), which are the day of year on which half of the annual precipitation and potential evapotranspiration have occurred, respectively. We find that CT_{PPT} is relatively invariant across the latitudinal transect, increasing by 6.5 days on average from south to north, with low variation (μ= 7 February ± 5.5 days), whereas CT_{PET} increases by 27 days on average from south to north with more variation (μ= 4 June ± 8.8 days). Moisture supply is therefore increasingly *out of phase* with energy demand with increasing latitude, driven by later dates of CT_{PET}. Consequently, the variability in *E* with latitude shown in Figure 4 is associated with variability in CT_{PET} more than CT_{PPT}.

Together, these patterns demonstrate that regional-scale differences in Q_{MIN} elasticity to climatic variability are associated with the degree to which moisture supply meets or exceeds energy demand (*P/PET*) as well as the degree to which moisture supply is in phase with energy demand. In the humid Pacific Northwest, where moisture supply exceeds (and is more out of phase with) energy demand, Q_{MIN} elasticity to winter and summer climate variability is lower. In California, energy demand generally exceeds (and is more in phase with) moisture supply, and Q_{MIN} elasticity to both winter and summer climate variability is substantially larger.

4.3. The Role of Snow Accumulation and Snowmelt Timing

Previous studies have identified spatial differences in the magnitude of snow accumulation and snowmelt timing as key drivers of summer streamflow sensitivity in the western United States (Fritze et al., 2011; Stewart et al., 2005). Here we test the relationship between *SWE/P* ratios and *E*, highlighting differences in this relationship between the northern (primarily humid) and southern (primarily semiarid) portions of our study area. The *SWE/P* ratio covaries with mean annual air temperature, both for catchments south of 40°N ($r = -0.94$, $p < 10^{-12}$) and north of 40°N ($r = -0.92$, $p < 10^{-35}$). Unlike the strong gradient in the humidity index from south to north along our transect, the range of mean annual air temperatures is nearly identical among catchments in the semiarid California mountains as compared with the humid Pacific Northwest mountains (~ −3 to 11 °C, not shown). The similar range of air temperature variability in both regions

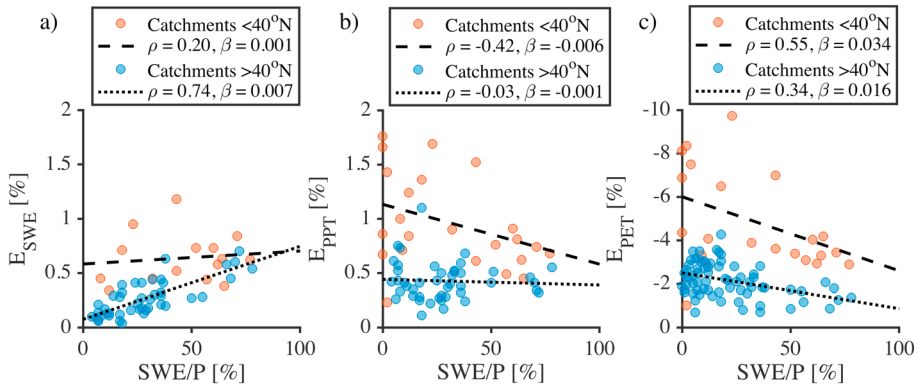

Figure 6. (a) E_{SWE}, (b) E_{PPT}, and (c) E_{PET} versus *SWE/P* for catchments with locally significant ($p \leq 0.05$) elasticity regressions. Spearman correlation coefficients ρ and slope β for dashed/dotted linear trend lines are shown for catchments located south/north of 40°N in the (primarily semiarid) California mountains and the (primarily humid) Pacific Northwest, respectively.

drives a similar range in *SWE/P* ratios, from rain-dominated catchments with *SWE/P* = 0 to snow-dominated catchments with *SWE/P* ratios approaching 90%.

We find that an increase in the *SWE/P* ratio is associated with reduced $|E_{PPT}|$ and $|E_{PET}|$ values in both California and the Pacific Northwest (Figures 6b and 6c), suggesting the proportional response of Q_{MIN} to climatic variability is lower in colder, snow-dominated catchments. Given the tight relationship between mean annual air temperatures and *SWE/P* ratios, relationships between *E* values and both elevation and air temperature mirror those with *SWE/P* (not shown). Among catchments in the semiarid California mountains, the *SWE/P* ratio mediates both E_{PPT} and E_{PET}, with a similar relative reduction in the magnitude of $|E|$ values and similar correlation for both variables (cf. Figure 6b to Figure 6c dashed lines). For catchments in the humid Pacific Northwest, the *SWE/P* ratio mediates E_{PET} but not E_{PPT} (cf. Figure 6b to Figure 6c dotted lines). In both regions, the reduction in $|E_{PPT}|$ and $|E_{PET}|$ values is most pronounced among catchments with *SWE/P* > ~30%.

Conversely, we find $|E_{SWE}|$ values increase with larger *SWE/P* ratios, in both California and the Pacific Northwest (Figure 6a). Whereas this means warmer catchments appear less sensitive to changes in *SWE*, this result fundamentally reflects the weaker correlation between Q_{MIN} and *SWE* in warm, low-elevation catchments where *SWE* is a smaller portion of the water balance. The decrease in $|E_{SWE}|$ with smaller *SWE/P* ratios reflects the diminishing influence of *SWE* on Q_{MIN} among catchments characterized by transient, mixed rain-snow, or rain-dominated precipitation regimes, whereas the increase in $|E_{PPT}|$ and $|E_{PET}|$ with smaller *SWE/P* ratios reflects the increase in Q_{MIN} variability relative to climatic variability among these catchments.

We found nearly identical relationships between *E* values and the mean annual date of SWE_{MAX} (*DPS*) as we found between *E* values and *SWE/P* (not shown). The *SWE/P* ratio and the *DPS* are strongly correlated in our study region (r = 0.81, $p < 10^{-26}$), suggesting that *SWE/P* is effectively a proxy for *DPS* and vice versa. In general, we found that catchments with the latest *DPS* are located in the humid Pacific Northwest, where later *DPS* is associated with lower $|E_{PET}|$ but not $|E_{PPT}|$, suggesting that snow cover in this region reduces the percent change in Q_{MIN} for a unit percent change in *PET* but has no effect on the percent change in Q_{MIN} for a unit percent change in *PPT*. This likely reflects the effect of longer snow cover duration on energy-limited conditions in this region. The reduction in $|E_{PET}|$ with larger *SWE/P* and later *DPS* suggests that snow cover reduces the effect of late spring and early summer evaporative losses on Q_{MIN}, whereas moisture supply during summer is less affected by the amount or duration of snow cover in the Pacific Northwest.

4.4. Elasticity in Rain- Versus Snow-Dominated Catchments

To further explore the effect of seasonal snow accumulation, we examine how the distribution of *E*, as well as *r* and S_Y/S_X (equation (2)), varies in rain- versus snow-dominated catchments. We examine *r* and S_Y/S_X separately to infer whether differences in *E* are related to the ratio of interannual Q_{MIN} variability to climatic variability (S_Y/S_X) versus the correlation between Q_{MIN} and climatic variability (*r*). On average, E_{PPT} is 0.70% in rain-dominated catchments versus 0.55% in snow-dominated catchments (Figure 7; Table 1). The smaller E_{PPT} in snow-dominated catchments is explained by a dampening of interannual Q_{MIN} variability relative to climatic

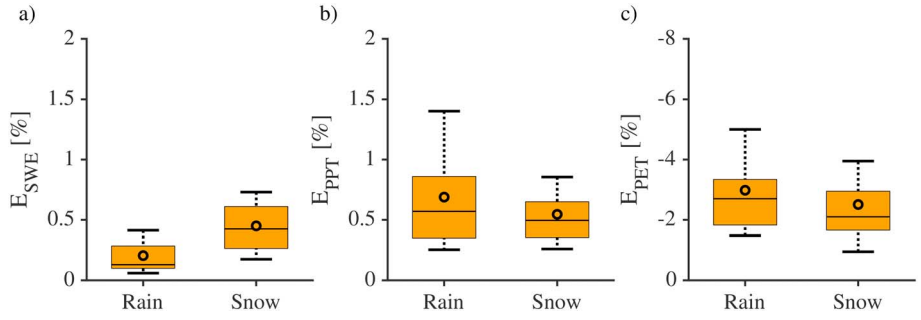

Figure 7. The distribution of (a) E_{SWE}, (b) E_{PPT}, and (c) E_{PET} for all catchments with locally significant ($p \leq 0.05$) elasticity regressions within the rain- versus snow-dominated precipitation regime categories. The line inside each boxplot is the median, the circle is the mean, the lower and upper box edges are the 25th and 75th percentiles, and the lower and upper whiskers are the 10th and 90th percentiles, respectively.

variability in these catchments. For example, correlation between Q_{MIN} and *PPT* is 0.56 and 0.54 for rain- and snow-dominated catchments, respectively (cf. $r_{Q_{MIN,PPT}}$, Table 1) but the ratio of interannual Q_{MIN} variability to interannual *PPT* variability is 1.2 and 1.0 for rain- and snow-dominated catchments, respectively (cf. $S_{Q_{MIN}}/S_{PPT}$, Table 1). This can be interpreted to say that, on average, the proportional response of Q_{MIN} to a unit of variability in *PPT* is smaller in snow-dominated catchments than in rain-dominated catchments.

Results for E_{PET} support the dampening effect of snow on *E*. On average, correlation between Q_{MIN} and *PET* is −0.53 and −0.54 for rain- and snow-dominated catchments, respectively (cf. $r_{Q_{MIN,PET}}$, Table 1), but the ratio of interannual Q_{MIN} variability to interannual *PET* variability is 5.9 and 4.5 for rain- and snow-dominated catchments, respectively (cf. $S_{Q_{MIN}}/S_{PET}$, Table 1). As with *PPT*, the correlation between Q_{MIN} and *PET* is relatively constant across precipitation regimes, whereas interannual Q_{MIN} variability relative to interannual *PET* variability is smaller in snow-dominated catchments. Relating this to section 4.3, this confirms that the reduction in $|E_{PPT}|$ and $|E_{PET}|$ values with larger *SWE*/*P* ratios (Figures 6b and 6c) is explained by a reduction in the proportional response of Q_{MIN} to climatic variability as opposed to systematic differences in correlation.

Table 1
Summary Statistics for Summer Minimum Streamflow (Q_{MIN}) Elasticity to Annual Maximum Snow Water Equivalent (E_{SWE}), Cumulative Winter Precipitation (E_{PPT}), and Cumulative Summer Potential Evapotranspiration (E_{PET})

Item	Rain-dominated catchments ($\alpha = 0.05$)	Snow-dominated catchments ($\alpha = 0.05$)	Fast-draining catchments ($\alpha = 0.05$)	Slow-draining catchments ($\alpha = 0.05$)	All catchments with significant correlation ($\alpha = 0.05$)	All catchments
E_{SWE}						
N ($\alpha = 0.05$)	21	40	24	37	61	110
Elasticity (%)	0.21	0.45	0.41	0.34	0.37	0.22
$r_{QMIN,SWE}$	0.42	0.57	0.51	0.53	0.52	0.35
S_{QMIN}/S_{SWE}	0.5	0.8	0.7	0.6	0.7	0.7
Elevation (m a.s.l.)	1,008	1,638	1,482	1,382	1,421	1,170
E_{PPT}						
N ($\alpha = 0.05$)	29	40	36	33	69	110
Elasticity (%)	0.70	0.55	0.76	0.44	0.61	0.45
$r_{QMIN,PPT}$	0.56	0.54	0.57	0.52	0.55	0.39
S_{QMIN}/S_{PPT}	1.2	1.0	1.4	0.9	1.1	1.2
Elevation (m a.s.l.)	1,003	1,641	1,324	1,428	1,373	1,159
E_{PET}						
N ($\alpha = 0.05$)	52	41	53	40	93	110
Elasticity (%)	−2.98	−2.51	−3.34	−2.02	−2.77	−2.5
$r_{QMIN,PET}$	−0.53	−0.54	−0.53	−0.54	−0.54	−0.48
S_{QMIN}/S_{PET}	5.9	4.5	6.5	3.7	5.3	5.3
Elevation (m a.s.l.)	783	1,612	1,099	1,215	1,149	1,159

Note. Where indicated, values in each category are averaged across catchments with locally significant ($\alpha = 0.05$) elasticity regressions. Elevation is the catchment median from GAGES-II. GAGES-II = Geospatial Attributes of Gages for Evaluating Streamflow, version II.

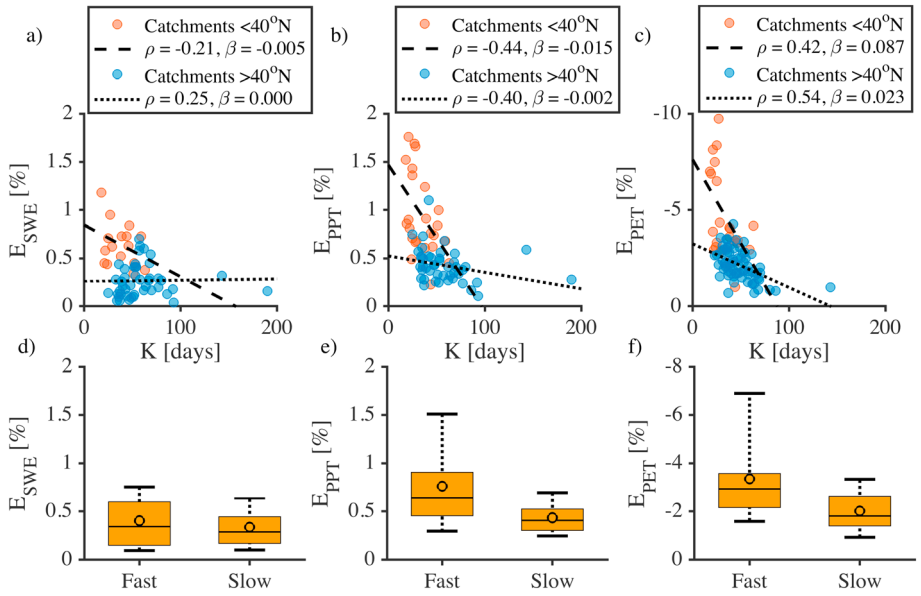

Figure 8. (a) E_{SWE}, (b) E_{PPT}, and (c) E_{PET} versus storage coefficients K for catchments with locally significant ($p \leq 0.05$) elasticity regressions. The storage coefficient is the characteristic time scale of baseflow recession; longer K suggests larger contributions of groundwater to baseflow. Spearman correlation coefficients ρ and slope β for dashed/dotted linear trend lines are shown for catchments located south/north of 40°N in the (primarily semiarid) California mountains and the (primarily humid) Pacific Northwest, respectively. The distribution of (d) E_{SWE}, (e) E_{PPT}, and (f) E_{PET} for all catchments with locally significant ($p \leq 0.05$) elasticity regressions within the fast-draining ($K < 45$ days) and slow-draining ($K \geq 45$ days) hydrologic regime categories. The line inside each boxplot is the median, the circle is the mean, the lower and upper box edges are the 25th and 75th percentiles, and the lower and upper whiskers are the 10th and 90th percentiles, respectively.

Conversely, $|E_{SWE}|$ is larger and more variable in snow-dominated catchments (Figure 7). This is not surprising because correlation between Q_{MIN} and SWE_{MAX} is considerably lower in the rain-dominated category (cf. $r_{Q_{MIN},SWE}$, Table 1). The smallest SWE/P ratio in the E_{SWE} rain-dominated category is 0.04; therefore, catchments in this category are characterized by a transient, mixed snow-rain precipitation regime. The smaller $|E_{SWE}|$ in this category fundamentally reflects the weak correlation between Q_{MIN} and SWE_{MAX} in rain-dominated catchments and also demonstrates the reduction in correlation between Q_{MIN} and SWE_{MAX} that results from a climatic shift from snow- to rain-dominated conditions. In general, the smaller $|E_{SWE}|$ in rain-dominated catchments reflects poor correlation between Q_{MIN} and SWE_{MAX} in these catchments, whereas the larger and more variable $|E_{PPT}|$ and $|E_{PET}|$ reflects the larger variability of Q_{MIN} relative to climatic variability in rain-dominated catchments.

4.5. Elasticity in Slow- Versus Fast-Draining Catchments

In addition to spatial differences in snow accumulation and snowmelt timing, spatial differences in drainage rates are known to mediate summer streamflow sensitivity to climate in our study area (Tague et al., 2008). Here storage coefficients K are used to infer the influence of drainage rates on E. Across the 110 catchments, we find K values average 48 ± 23 days (±1 standard deviation), with median 43 days and range 18–190 days. Brutsaert (2008, 2010) found that K averaged 45 ± 14 days for a set of river basins in the central and eastern United States, whereas Sánchez-Murillo et al. (2015) found that K averaged 33 ± 15 days for 26 catchments in eastern Washington and Idaho. K values vary with catchment size, slope, and aridity, which may explain the larger range and variability of K values we find (Tague & Grant, 2009). In total, 59 catchments were classified as fast draining ($K < 45$ days) and 51 catchments as slow draining ($K \geq 45$ days), with mean R^2 of 0.69 and 0.48 for their $|dQ/dt|$ versus Q regressions, respectively.

We find that $|E|$ values decrease with larger K values, suggesting that the proportional response of Q_{MIN} to climatic variability is lower in slow-draining catchments with protracted baseflow recession (Figure 8). Among catchments in the semiarid California mountains, there is a strong reduction in $|E_{PPT}|$ and $|E_{PET}|$ with larger K values but no statistically significant relationship between E_{SWE} and K. Among catchments north of

40°N in the humid Pacific Northwest, K appears to mediate E_{PET} more than E_{PPT} (which was also found for the snow metrics SWE/P and DPS), whereas the relationship between E_{SWE} and K is statistically insignificant (Figure 8a dotted line). Though correlations between E_{SWE} and K were not found, correlations between E_{PPT}, E_{PET}, and K were stronger in snow-dominated catchments (not shown). Together, these results suggest that percent changes in Q_{MIN} relative to percent changes in PPT and PET are lower in slow-draining catchments, and this dampening effect is strongest in snow-dominated catchments.

Differences in E values are stark when averaged across all catchments in the fast- and slow-draining hydrologic regime categories (Figures 8d–8f and Table 1). On average, $|E_{SWE}|$, $|E_{PPT}|$, and $|E_{PET}|$ are each smaller and less variable in slow-draining catchments than in fast-draining catchments. As with precipitation regime, differences in E across hydrologic regime are explained by differences in interannual Q_{MIN} variability relative to climatic variability. The ratio of interannual Q_{MIN} variability to interannual variability in SWE_{MAX}, PPT, and PET is lower in slow-draining catchments than in fast-draining catchments for each variable, whereas correlations are nearly identical (cf. r and S_Y/S_X in slow- versus fast-draining catchments, Table 1). However, differences in E across hydrologic regime are larger than differences in E across precipitation regime. Together, the smallest $|E_{PPT}|$ and $|E_{PET}|$ are found in slow-draining catchments that are also snow dominated, whereas the smallest $|E_{SWE}|$ are found in slow-draining catchments that are also rain dominated, although this latter effect is due to the poor correlation between Q_{MIN} and SWE in rain-dominated catchments.

Given the strong relationships between K values and E values for all variables, it is important to determine whether K values are proxies for catchment climatic or physiographic factors. We find no statistically significant correlation between K values and relief ratio, mean catchment slope, catchment drainage area, stream density, stream order, catchment compactness index, or mean catchment elevation. K values were, however, positively correlated ($r = 0.59$, $p < 10^{-13}$) with the baseflow index metric included in the GAGES-II database. Baseflow index is the ratio of baseflow to annual streamflow and is broadly representative of the influence of groundwater contributions to streamflow (Wolock, 2003); therefore, we expect this metric to be positively correlated with our K values. We find no statistically significant correlation between K values and climatic factors including mean annual runoff and mean annual PPT. K values were, however, negatively correlated with mean annual air temperature ($r = -0.31$, $p < 10^{-3}$) and mean annual PET ($r = -0.27$, $p < 10^{-2}$) and were positively correlated with DPS ($r = 0.36$, $p < 10^{-4}$), SWE_{MAX} ($r = 0.28$, $p < 10^{-2}$) and latitude ($r = 0.28$, $p < 10^{-2}$). These correlations suggest that colder catchments, which have less PET, more SWE, and later DPS, also tend to be categorized as slow draining and also that higher latitude catchments, which tend to have smaller P/PET, tend to be categorized as slow-draining catchments.

5. Discussion

5.1. Summer Low-Flow Elasticity to Winter Precipitation Compared to Summer Evaporative Demand

Absolute values of summer low-flow (Q_{MIN}) elasticity to summer evaporative demand (PET) are approximately 4–5 times larger than to winter precipitation (PPT) or annual maximum SWE (SWE_{MAX}), with median elasticities of −2.1%, 0.50%, and 0.43% for catchments where SWE_{MAX} exceeds 20% of the annual precipitation, respectively. Underlying this, we find that correlations between Q_{MIN} and SWE_{MAX}, PPT, and PET are nearly identical, but for every unit of variation in PET, the corresponding unit of variation in Q_{MIN} is approximately 4–5 times larger than for SWE_{MAX} or PPT. Given the nearly identical correlations, this suggests that variability in PET exerts a stronger control on variability in Q_{MIN} than in PPT and also that variability in PET is small relative to variability in PPT. In addition, Q_{MIN} elasticity to climatic variability is substantially larger in semiarid catchments than in humid catchments. These findings both support the notion that small changes in PET or the ratio P/PET have the potential to drive large changes in Q_{MIN} and its elasticity to climatic variability in the western United States, especially where evaporative demand is seasonally in phase with moisture supply.

The implication of these findings for low flows in a changing climate depends on both the magnitude of change in the proximate forcing variables and the magnitude of the elasticities we document. A large change in PPT combined with a small elasticity to PPT could outweigh a small change in PET combined with a large elasticity to PET (Tan & Gan, 2015). In addition, our elasticities may not describe the response of low flows to changes in PPT and PET outside their historic variability. The

assumption that increased *PET* leads to decreased streamflow is directly tied to the assumption that increased *PET* leads to increased actual evapotranspiration. Near-term increases in net surface radiation due to enhanced downwelling longwave radiation from a warmer atmosphere are expected to contribute primarily to warming of the surface air temperature as opposed to increased actual evapotranspiration (Roderick et al., 2014, 2015). Estimates of actual evapotranspiration are sparse, but historical data from the northern portion of our study region appear to support this. For example, trends in precipitation explain the majority of variability in annual and summer streamflow trends in the Pacific Northwest during the twentieth century, whereas trends in water-equivalent energy available for evapotranspiration are small in comparison (Jung et al., 2013; Kormos et al., 2016; Luce et al., 2013). Kormos et al. (2016) provide a cogent discussion of these issues, arguing low flows in the Pacific Northwest have likely not been affected by increased evapotranspiration despite an increase in the regional air temperature and growing season evaporative demand (Abatzoglou et al., 2013), but in principle, their arguments apply to annual not seasonal flows (Kumar et al., 2013; Roderick et al., 2014).

The response of seasonal streamflow including summer low flows to increased evaporative demand has received less attention. Evidence from the Sierra Nevada mountains suggests that actual evapotranspiration may scale with evaporative demand and reduce dry season streamflow in catchments where growing season length and spatial extent is cold limited and vegetation rooting depth has access to deeper water storage in decomposed regolith (Bales et al., 2011; Goulden & Bales, 2014; Klos et al., 2018). This latter point is relevant to our analysis of slow- versus fast-draining catchments. Although we find that slow-draining catchments have lower elasticity on average and therefore appear less sensitive, these same catchments have more subsurface water storage in late summer available for extraction and therefore may be more vulnerable to increased evaporative demand (Jepsen et al., 2016; Tague, 2009). Future work should aim to isolate the mechanisms that control the seasonal partitioning of precipitation into evapotranspiration versus streamflow during periods of increased evaporative demand, for example, using modeling experiments (Foster et al., 2016) or during extreme events such as the recent California drought (Bales et al., 2018).

5.2. Summer Low-Flow Elasticity in Rain- Versus Snow-Dominated Catchments

We find that summer low-flow elasticity to the annual maximum SWE (SWE_{MAX}) ranges from 0.13% to 1.18% (median 0.43%), similar to values reported for the Sierra Nevada mountains and the Swiss Alps (Godsey et al., 2014; Jenicek et al., 2016, 2018). The magnitude of low-flow elasticity to SWE_{MAX} depends on the correlation between low flows and SWE_{MAX}. Warmer, lower elevation catchments with low *SWE*/*P* ratios have lower correlation and consequently lower elasticity. Whereas this suggests lower sensitivity, catchments dominated by low- and middle-elevation *snow at risk* are likely to experience the largest near-term declines in SWE_{MAX} in a warming climate (Nolin & Daly, 2006; Tennant et al., 2015). Low-flow vulnerability to changes in SWE_{MAX} is therefore likely to follow the region- and elevation-specific climate sensitivity of catchment snowpack, whereas the differences between low-flow elasticities in rain- versus snow-dominated catchments we document demonstrate the diminishing influence (and predictive utility) of SWE_{MAX} on summer low flows if catchments shift from snow- to rain-dominated conditions (Jenicek et al., 2018).

Low-flow elasticity to SWE_{MAX} is also clearly not independent of low-flow elasticity to *PPT*. To explore this interdependence indirectly, we compared low-flow elasticity to *PPT* and *PET* in snow- versus rain-dominated catchments. Applying this *space for time* transformation, we infer that rain-dominated catchments are more sensitive (have larger elasticity) to *PPT* and *PET* than snow-dominated catchments, on average. In the primarily energy-limited Pacific Northwest, larger *SWE*/*P* ratios are associated with reduced low-flow elasticity to *PET* but not *PPT*. In the primarily water-limited California mountains, larger *SWE*/*P* ratios are associated with reduced low-flow elasticity to both *PET* and *PPT*. This finding supports the notion that, in addition to providing an important moisture source (particularly in water-limited systems), snow cover increases runoff production by reducing atmospheric moisture losses (Bosson et al., 2012; Foster et al., 2016), shedding some light on the importance of *SWE* independently of *PPT* and its role in controlling seasonal impacts to low flows in a warming climate. Moreover, these findings suggest that a shift from snow- to rain-dominated conditions may lead to lower low flows and enhanced variability in low flows in response to a decline in *PPT* or an increase in *PET* than expected in the absence of declining *SWE*. Teasing out the underlying causal factors of these nonlinear effects should continue to receive attention (e.g., Barnhart et al., 2016).

5.3. Summer Low-Flow Elasticity in Slow- Versus Fast-Draining Catchments

Absolute values of summer low-flow elasticity to SWE_{MAX}, *PPT*, and *PET* are lower in slow-draining catchments than in fast-draining catchments, highlighting the importance of catchment physiographic factors such as soil and rock porosity and permeability and catchment size, shape, and slope in controlling summer streamflow and its response to climate variability (Cummings & Eibert, 2018; Jepsen et al., 2016; Klos et al., 2014; Lovill et al., 2018; Tague & Grant, 2009). As with larger *SWE*/*P* ratios, the slow release of catchment water storage reduces the interannual variability of low flows relative to climatic variability in both semiarid and humid catchments, but the mediating effect of drainage rates is stronger than the *SWE*/*P* ratio effect. On average, elasticity to *PPT* and *PET* is lower by 0.32% and 1.3%, respectively, in slow-draining catchments than fast-draining catchments, compared to 0.15% and 0.47% respective reductions in snow-dominated catchments versus rain-dominated catchments.

We also find that storage coefficients are negatively correlated with SWE_{MAX}. In addition to catchment geology, storage coefficients integrate effects of shallow subsurface hydrology and root-zone soil moisture dynamics on baseflow recession (Bart & Tague, 2017). Smaller snowpacks that melt earlier have slower snowmelt rates (Musselman et al., 2017), which are hypothesized to decrease runoff generation owing to less efficient snowmelt infiltration into subsurface storage below the root-zone that sustains dry season runoff (Barnhart et al., 2016). Larger, faster-melting snowpacks may therefore lead to slower baseflow recessions owing to more efficient snowmelt infiltration into subsurface storage and/or less atmospheric moisture loss.

Although these results suggest that slow-draining catchments are the least sensitive to climatic variability, elasticities represent the percent change in Q_{MIN} with respect to unit percent changes in climatic forcing. Absolute declines in Q_{MIN} may be larger in slow-draining catchments where mean summer flows are large relative to fast-draining catchments (Safeeq et al., 2013; Tague et al., 2008; Tague & Grant, 2009). Similarly, large percent changes in Q_{MIN} in fast-draining catchments may be small in absolute terms relative to historic variability. In these catchments, water management infrastructure and decision making may have adapted to historically large interannual streamflow variability and may be less vulnerable to large percent changes in low flows (Tague & Grant, 2009). Future work should identify the implications of relative versus absolute changes in summer streamflow for the range of stakeholder interests in the western United States (Tague et al., 2008) and assess whether hydrologic models in use today capture the complex interactions between snowmelt, subsurface hydrology, and seasonal streamflow generation that explain the elasticity patterns identified here (Jepsen et al., 2016; Markovich et al., 2016; Maxwell & Condon, 2016; Tague et al., 2013).

5.4. Limitations of This Study and Future Research Needs

Our results pertain to the magnitude of low flows and not their timing or duration. Our results suggest that low-flow elasticity to SWE_{MAX} is lower than to *PPT* and *PET*, but reductions in SWE_{MAX} could dominate impacts to aquatic habitats that depend on the consistency and temperature-mediating effect of snowmelt recharge (Arismendi et al., 2013; Mantua et al., 2010). We use a bivariate parametric estimator of elasticity that assumes that SWE_{MAX}, *PPT*, and *PET* are independent. Multivariate regression may provide more robust estimates of annual and low-flow elasticity to multiple sources of climatic variability (Kormos et al., 2016; Tsai, 2017). We do not address persistence (memory) in the annual time series of low flows and climate variables, nor do we address dependence of elasticity on hydrologic memory (Godsey et al., 2014; Jefferson et al., 2008). The maritime western United States is characterized by prolonged multiyear drought followed by sudden recovery (Dettinger, 2013), which may become more extreme in a future climate (Francis & Vavrus, 2012). Understanding the role of antecedent conditions and the degree to which changes in precipitation or evaporative demand will exacerbate or mitigate low-flow vulnerability to changes in snow accumulation and melt should remain imperatives (Bales et al., 2018; Luce et al., 2013).

6. Conclusions

Three clear patterns emerge from our analysis of summer low-flow elasticity to climatic variability in the maritime western U.S. mountains:

1. Low-flow elasticity to summer evaporative demand is 4–5 times larger on an absolute basis than elasticity to winter precipitation and annual maximum SWE. In addition, low-flow elasticity to annual maximum SWE, winter precipitation, and summer evaporative demand is larger and more variable in the semiarid

California mountains than in the humid Pacific Northwest. These findings both support the notion that small changes in evaporative demand have the potential to drive large changes in low flows and their elasticity to climatic variability in the western United States if low flows maintain their historic relationship to evaporative demand.

2. Low-flow elasticity to winter precipitation and summer evaporative demand is lower on an absolute basis for snow-dominated catchments than for rain-dominated catchments. In the humid Pacific Northwest, snow reduces low-flow elasticity to summer evaporative demand but not to winter precipitation, whereas in the semiarid California mountains, snow reduces low-flow elasticity to both winter precipitation and summer evaporative demand. In the event of continued reductions of annual maximum SWE and earlier snowmelt timing across the western United States, these results suggest that low flows in snow-dominated catchments are likely to become lower, more variable, and less predictable in the future.
3. Low-flow elasticity to annual maximum SWE, winter precipitation, and summer evaporative demand is markedly lower for slow-draining catchments where the baseflow recession process is strongly controlled by seasonal changes in groundwater storage. This effect is found for all variables examined, is independent of latitude, and is stronger than the effect of rain versus snow precipitation regime. Low-flow variability is smallest in slow-draining catchments, and the proportional response of low flows to climate variability and change is likely to be smallest in slow-draining catchments.

Our results provide broad insight into the factors that control spatial variability in the climatic sensitivity of low flows in the maritime western U.S. mountains. In general, catchments in the semiarid California mountains are highly sensitive to climatic variability, and this sensitivity is lower where SWE is a larger portion of annual precipitation. Catchments in the humid Pacific Northwest are less sensitive to climatic variability, but as with California, sensitivity is lower where annual maximum SWE is a larger portion of annual precipitation. In both regions, low flows are more sensitive to summer evaporative demand than annual maximum SWE or winter precipitation. However, this should be balanced against the larger expected near-term changes in future SWE. If precipitation magnitude and evapotranspiration do not change substantially, low- and middle-elevation snow-dominated catchments with catchment geology that favors fast baseflow recession are likely to experience the largest near-term percent declines in low flows in a warming climate.

Acknowledgments
The authors declare no real or perceived financial conflicts of interests. The authors thank James Kirchner of ETH Zürich for his time and discussions that contributed to the research questions addressed by this work. The data presented in this manuscript are available in the supporting information. The source data used are available from the GAGES-II data set (Falcone, 2011) and the Livneh et al. (2015) data set.

References

Abatzoglou, J. T., Rupp, D. E., & Mote, P. W. (2013). Seasonal climate variability and change in the Pacific Northwest of the United States. *Journal of Climate*, *27*(5), 2125–2142. https://doi.org/10.1175/JCLI-D-13-00218.1

Allen, R. G., Pereira, L. S., Raes, D., & Smith, M. (1998). Crop evapotranspiration—Guidelines for computing crop water requirements—FAO irrigation and drainage paper 56. *FAO, Rome*, *300*(9), D05109.

Arismendi, I., Safeeq, M., Johnson, S. L., Dunham, J. B., & Haggerty, R. (2013). Increasing synchrony of high temperature and low flow in western North American streams: Double trouble for coldwater biota? *Hydrobiologia*, *712*(1), 61–70. https://doi.org/10.1007/s10750-012-1327-2

Bales, R. C., Goulden, M. L., Hunsaker, C. T., Conklin, M. H., Hartsough, P. C., O'Geen, A. T., et al. (2018). Mechanisms controlling the impact of multi-year drought on mountain hydrology. *Scientific Reports*, *8*(1), 690. https://doi.org/10.1038/s41598-017-19007-0

Bales, R. C., Hopmans, J. W., O'Geen, A. T., Meadows, M., Hartsough, P. C., Kirchner, P., et al. (2011). Soil moisture response to snowmelt and rainfall in a Sierra Nevada mixed-conifer forest. *Vadose Zone Journal*, *10*(3), 786–799. https://doi.org/10.2136/vzj2011.0001

Barnhart, T. B., Molotch, N. P., Livneh, B., Harpold, A. A., Knowles, J. F., & Schneider, D. (2016). Snowmelt rate dictates streamflow. *Geophysical Research Letters*, *43*, 8006–8016. https://doi.org/10.1002/2016GL069690

Bart, R. R., & Tague, C. L. (2017). The impact of wildfire on baseflow recession rates in California. *Hydrological Processes*, *31*(8), 1662–1673. https://doi.org/10.1002/hyp.11141

Berghuijs, W. R., Larsen, J. R., van Emmerik, T. H. M., & Woods, R. A. (2017). A global assessment of runoff sensitivity to changes in precipitation, potential evaporation, and other factors. *Water Resources Research*, *53*, 8475–8486. https://doi.org/10.1002/2017WR021593

Berghuijs, W. R., Hartmann, A., & Woods, R. A. (2016). Streamflow sensitivity to water storage changes across Europe. *Geophysical Research Letters*, *43*, 1980–1987. https://doi.org/10.1002/2016GL067927

Berghuijs, W. R., Woods, R. A., & Hrachowitz, M. (2014). A precipitation shift from snow towards rain leads to a decrease in streamflow. *Nature Climate Change*, *4*(7), 583–586. https://doi.org/10.1038/nclimate2246

Bosson, E., Sabel, U., Gustafsson, L., Sassner, M., & Destouni, G. (2012). Influences of shifts in climate, landscape, and permafrost on terrestrial hydrology. *Journal of Geophysical Research*, *117*, D05120. https://doi.org/10.1029/2011JD016429

Brutsaert, W. (2008). Long-term groundwater storage trends estimated from streamflow records: Climatic perspective. *Water Resources Research*, *44*, W02409. https://doi.org/10.1029/2007WR006518

Brutsaert, W. (2010). Annual drought flow and groundwater storage trends in the eastern half of the United States during the past two-third century. *Theoretical and Applied Climatology*, *100*(1–2), 93–103. https://doi.org/10.1007/s00704-009-0180-3

Brutsaert, W., & Nieber, J. L. (1977). Regionalized drought flow hydrographs from a mature glaciated plateau. *Water Resources Research*, *13*(3), 637–643. https://doi.org/10.1029/WR013i003p00637

Budyko, M. I. (Ed.) (1974). VI climatic factors of geographical zonality. In *International geophysics* (Vol. 18, pp. 317–370). New York: Academic Press. https://doi.org/10.1016/S0074-6142(09)60011-5

Cummings, M. L., & Eibert, D. A. (2018). Winter rain versus snow in headwater catchments: Responses of an unconfined pumice aquifer, south-central Oregon, USA. *Journal of Water Resource and Protection*, *10*(04), 461–492. https://doi.org/10.4236/jwarp.2018.104025

Dettinger, M. D. (2013). Atmospheric rivers as drought busters on the U.S. West Coast. *Journal of Hydrometeorology*, *14*(6), 1721–1732. https://doi.org/10.1175/JHM-D-13-02.1

Dooge, J. C. I. (1992). Sensitivity of runoff to climate change: A Hortonian approach. *Bulletin of the American Meteorological Society*, *73*(12), 2013–2024. https://doi.org/10.1175/1520-0477(1992)073<2013:SORTCC>2.0.CO;2

Falcone, J. A. (2011). *GAGES-II: Geospatial attributes of gages for evaluating streamflow (USGS unnumbered series)*. Reston, VA: U.S. Geological Survey. Retrieved from http://pubs.er.usgs.gov/publication/70046617

Falcone, J. A., Carlisle, D. M., Wolock, D. M., & Meador, M. R. (2010). GAGES: A stream gage database for evaluating natural and altered flow conditions in the conterminous United States. *Ecology*, *91*(2), 621–621. https://doi.org/10.1890/09-0889.1

Foster, L. M., Bearup, L. A., Molotch, N. P., Brooks, P. D., & Maxwell, R. M. (2016). Energy budget increases reduce mean streamflow more than snow–rain transitions: Using integrated modeling to isolate climate change impacts on Rocky Mountain hydrology. *Environmental Research Letters*, *11*(4), 044015. https://doi.org/10.1088/1748-9326/11/4/044015

Francis, J. A., & Vavrus, S. J. (2012). Evidence linking Arctic amplification to extreme weather in mid-latitudes. *Geophysical Research Letters*, *39*, L06801. https://doi.org/10.1029/2012GL051000

Fritze, H., Stewart, I. T., & Pebesma, E. (2011). Shifts in western North American snowmelt runoff regimes for the recent warm decades. *Journal of Hydrometeorology*, *12*(5), 989–1006. https://doi.org/10.1175/2011JHM1360.1

Gergel, D. R., Nijssen, B., Abatzoglou, J. T., Lettenmaier, D. P., & Stumbaugh, M. R. (2017). Effects of climate change on snowpack and fire potential in the western USA. *Climatic Change*, *141*(2), 287–299. https://doi.org/10.1007/s10584-017-1899-y

Godsey, S. E., Kirchner, J. W., & Tague, C. L. (2014). Effects of changes in winter snowpacks on summer low flows: Case studies in the Sierra Nevada, California, USA. *Hydrological Processes*, *28*(19), 5048–5064. https://doi.org/10.1002/hyp.9943

Goulden, M. L., & Bales, R. C. (2014). Mountain runoff vulnerability to increased evapotranspiration with vegetation expansion. *Proceedings of the National Academy of Sciences*, *111*(39), 14071–14075. https://doi.org/10.1073/pnas.1319316111

Hamlet, A. F., Huppert, D., & Lettenmaier, D. P. (2002). Economic value of long-lead streamflow forecasts for Columbia River hydropower. *Journal of Water Resources Planning and Management*, *128*(2), 91–101. https://doi.org/10.1061/(ASCE)0733-9496(2002)128:2(91)

Harman, C. J., Troch, P. A., & Sivapalan, M. (2011). Functional model of water balance variability at the catchment scale: 2. Elasticity of fast and slow runoff components to precipitation change in the continental United States. *Water Resources Research*, *47*, W02523. https://doi.org/10.1029/2010WR009656

Howitt, R. E., MacEwan, D., Medellín-Azuara, J., Lund, J. R., & Sumner, D. A. (2015). *Economic analysis of the 2015 drought for California agriculture*. University of California, Davis: Center for Watershed Sciences.

Jaeger, W. K., Amos, A., Bigelow, D. P., Chang, H., Conklin, D. R., Haggerty, R., et al. (2017). Finding water scarcity amid abundance using human–natural system models. *Proceedings of the National Academy of Sciences*, *114*(45), 11884–11889. https://doi.org/10.1073/pnas.1706847114

Jefferson, A., Nolin, A., Lewis, S., & Tague, C. (2008). Hydrogeologic controls on streamflow sensitivity to climate variation. *Hydrological Processes*, *22*(22), 4371–4385. https://doi.org/10.1002/hyp.7041

Jenicek, M., Seibert, J., & Staudinger, M. (2018). Modeling of future changes in seasonal snowpack and impacts on summer low flows in alpine catchments. *Water Resources Research*, *54*, 538–556. https://doi.org/10.1002/2017WR021648

Jenicek, M., Seibert, J., Zappa, M., Staudinger, M., & Jonas, T. (2016). Importance of maximum snow accumulation for summer low flows in humid catchments. *Hydrology and Earth System Sciences*, *20*(2), 859–874. https://doi.org/10.5194/hess-20-859-2016

Jepsen, S. M., Harmon, T. C., Meadows, M. W., & Hunsaker, C. T. (2016). Hydrogeologic influence on changes in snowmelt runoff with climate warming: Numerical experiments on a mid-elevation catchment in the Sierra Nevada, USA. *Journal of Hydrology*, *533*, 332–342. https://doi.org/10.1016/j.jhydrol.2015.12.010

Jeton, A. E., Dettinger, M. D., & Smith, J. L. (1996). Potential effects of climate change on streamflow, eastern and western slopes of the Sierra Nevada, California and Nevada. US Department of the Interior, US Geological Survey.

Jung, I. W., Chang, H., & Risley, J. (2013). Effects of runoff sensitivity and catchment characteristics on regional actual evapotranspiration trends in the conterminous US. *Environmental Research Letters*, *8*(4), 044002. https://doi.org/10.1088/1748-9326/8/4/044002

Khaliq, M. N., Ouarda, T. B. M. J., Gachon, P., Sushama, L., & St-Hilaire, A. (2009). Identification of hydrological trends in the presence of serial and cross correlations: A review of selected methods and their application to annual flow regimes of Canadian rivers. *Journal of Hydrology*, *368*(1-4), 117–130. https://doi.org/10.1016/j.jhydrol.2009.01.035

Klos, P. Z., Goulden, M. L., Riebe, C. S., Tague, C. L., O'Geen, A. T., Flinchum, B. A., et al. (2018). Subsurface plant-accessible water in mountain ecosystems with a Mediterranean climate. *Wiley Interdisciplinary Reviews Water*, *5*(3), e1277. https://doi.org/10.1002/wat2.1277

Klos, P. Z., Link, T. E., & Abatzoglou, J. T. (2014). Extent of the rain-snow transition zone in the western U.S. under historic and projected climate. *Geophysical Research Letters*, *41*, 4560–4568. https://doi.org/10.1002/2014GL060500

Kormos, P. R., Luce, C. H., Wenger, S. J., & Berghuijs, W. R. (2016). Trends and sensitivities of low streamflow extremes to discharge timing and magnitude in Pacific Northwest mountain streams. *Water Resources Research*, *52*, 4990–5007. https://doi.org/10.1002/2015WR018125

Kumar, S., Lawrence, D. M., Dirmeyer, P. A., & Sheffield, J. (2013). Less reliable water availability in the 21st century climate projections. *Earth's Future*, *2*(3), 152–160. https://doi.org/10.1002/2013EF000159

Liang, X., Lettenmaier, D. P., Wood, E. F., & Burges, S. J. (1994). A simple hydrologically based model of land surface water and energy fluxes for general circulation models. *Journal of Geophysical Research*, *99*(D7), 14415–14,428. https://doi.org/10.1029/94JD00483

Lins, H. F., & Slack, J. R. (1999). Streamflow trends in the United States. *Geophysical Research Letters*, *26*(2), 227–230. https://doi.org/10.1029/1998GL900291

Livneh, B., Bohn, T. J., Pierce, D. W., Munoz-Arriola, F., Nijssen, B., Vose, R., et al. (2015). A spatially comprehensive, hydrometeorological data set for Mexico, the U.S., and Southern Canada 1950–2013. *Scientific Data*, *2*, 150042. https://doi.org/10.1038/sdata.2015.42

Lovill, S. M., Hahm, W. J., & Dietrich, W. E. (2018). Drainage from the critical zone: Lithologic controls on the persistence and spatial extent of wetted channels during the summer dry season. *Water Resources Research*. https://doi.org/10.1029/2017WR021903

Luce, C. H., Abatzoglou, J. T., & Holden, Z. A. (2013). The missing mountain water: Slower westerlies decrease orographic enhancement in the Pacific Northwest USA. *Science*, *342*(6164), 1360–1364. https://doi.org/10.1126/science.1242335

Mao, Y., Nijssen, B., & Lettenmaier, D. P. (2015). Is climate change implicated in the 2013–2014 California drought? A hydrologic perspective. *Geophysical Research Letters*, *42*, 2805–2813. https://doi.org/10.1002/2015GL063456

Mantua, N., Tohver, I., & Hamlet, A. (2010). Climate change impacts on streamflow extremes and summertime stream temperature and their possible consequences for freshwater salmon habitat in Washington state. *Climatic Change*, *102*(1–2), 187–223. https://doi.org/10.1007/s10584-010-9845-2

Markovich, K. H., Maxwell, R. M., & Fogg, G. E. (2016). Hydrogeological response to climate change in alpine hillslopes. *Hydrological Processes*, *30*(18), 3126–3138. https://doi.org/10.1002/hyp.10851

Maxwell, R. M., & Condon, L. E. (2016). Connections between groundwater flow and transpiration partitioning. *Science*, *353*(6297), 377–380. https://doi.org/10.1126/science.aaf7891

Milly, P. C. D. (1994). Climate, soil water storage, and the average annual water balance. *Water Resources Research*, *30*(7), 2143–2156. https://doi.org/10.1029/94WR00586

Milly, P. C. D., Kam, J., & Dunne, K. A. (2018). On the sensitivity of annual streamflow to air temperature. *Water Resources Research*, *54*, 2624–2641. https://doi.org/10.1002/2017WR021970

Mote, P. W., Li, S., Lettenmaier, D. P., Xiao, M., & Engel, R. (2018). Dramatic declines in snowpack in the western US. *Npj Climate and Atmospheric Science*, *1*(1), 2. https://doi.org/10.1038/s41612-018-0012-1

Musselman, K. N., Clark, M. P., Liu, C., Ikeda, K., & Rasmussen, R. (2017). Slower snowmelt in a warmer world. *Nature Climate Change*, *7*(3), 214–219. https://doi.org/10.1038/nclimate3225

Nolin, A. W., & Daly, C. (2006). Mapping "at risk" snow in the Pacific Northwest. *Journal of Hydrometeorology*, *7*(5), 1164–1171. https://doi.org/10.1175/JHM543.1

Rice, J. S., Emanuel, R. E., Vose, J. M., & Nelson, S. A. C. (2015). Continental U.S. streamflow trends from 1940 to 2009 and their relationships with watershed spatial characteristics. *Water Resources Research*, *51*, 6262–6275. https://doi.org/10.1002/2014WR016367

Risbey, J. S., & Entekhabi, D. (1996). Observed Sacramento Basin streamflow response to precipitation and temperature changes and its relevance to climate impact studies. *Journal of Hydrology*, *184*(3-4), 209–223. https://doi.org/10.1016/0022-1694(95)02984-2

Roderick, M. L., Greve, P., & Farquhar, G. D. (2015). On the assessment of aridity with changes in atmospheric CO_2. *Water Resources Research*, *51*, 5450–5463. https://doi.org/10.1002/2015WR017031

Roderick, M. L., Sun, F., Lim, W. H., & Farquhar, G. D. (2014). A general framework for understanding the response of the water cycle to global warming over land and ocean. *Hydrology and Earth System Sciences*, *18*(5), 1575–1589. https://doi.org/10.5194/hess-18-1575-2014

Rupp, D. E., & Selker, J. S. (2006a). Information, artifacts, and noise in $dQ/dt - Q$ recession analysis. *Advances in Water Resources*, *29*(2), 154–160. https://doi.org/10.1016/j.advwatres.2005.03.019

Rupp, D. E., & Selker, J. S. (2006b). On the use of the Boussinesq equation for interpreting recession hydrographs from sloping aquifers. *Water Resources Research*, *42*, W12421. https://doi.org/10.1029/2006WR005080

Safeeq, M., Grant, G. E., Lewis, S. L., Kramer, M. G., & Staab, B. (2014). A hydrogeologic framework for characterizing summer streamflow sensitivity to climate warming in the Pacific Northwest, USA. *Hydrology and Earth System Sciences*, *18*(9), 3693–3710. https://doi.org/10.5194/hess-18-3693-2014

Safeeq, M., Grant, G. E., Lewis, S. L., & Tague, C. L. (2013). Coupling snowpack and groundwater dynamics to interpret historical streamflow trends in the western United States. *Hydrological Processes*, *27*(5), 655–668. https://doi.org/10.1002/hyp.9628

Sánchez-Murillo, R., Brooks, E. S., Elliot, W. J., Gazel, E., & Boll, J. (2015). Baseflow recession analysis in the inland Pacific Northwest of the United States. *Hydrogeology Journal*, *23*(2), 287–303. https://doi.org/10.1007/s10040-014-1191-4

Sankarasubramanian, A., Vogel, R. M., & Limbrunner, J. F. (2001). Climate elasticity of streamflow in the United States. *Water Resources Research*, *37*(6), 1771–1781. https://doi.org/10.1029/2000WR900330

Schaake, J. C. (1990). From climate to flow. In P. E. Waggoner (Ed.), *Climate change and U.S. water resources* (pp. 177–206). New York, USA: John Wiley and Sons Inc.

Shukla, S., Safeeq, M., AghaKouchak, A., Guan, K., & Funk, C. (2015). Temperature impacts on the water year 2014 drought in California. *Geophysical Research Letters*, *42*, 4384–4393. https://doi.org/10.1002/2015GL063666

Stewart, I. T., Cayan, D. R., & Dettinger, M. D. (2005). Changes toward earlier streamflow timing across western North America. *Journal of Climate*, *18*(8), 1136–1155. https://doi.org/10.1175/JCLI3321.1

Tague, C. L. (2009). Assessing climate change impacts on alpine stream-flow and vegetation water use: Mining the linkages with subsurface hydrologic processes. *Hydrological Processes*, *23*(12), 1815–1819. https://doi.org/10.1002/hyp.7288

Tague, C. L., Choate, J. S., & Grant, G. E. (2013). Parameterizing sub-surface drainage with geology to improve modeling streamflow responses to climate in data limited environments. *Hydrology and Earth System Sciences*, *17*(1), 341–354. https://doi.org/10.5194/hess-17-341-2013

Tague, C. L., & Dugger, A. L. (2010). Ecohydrology and climate change in the mountains of the western USA—A review of research and opportunities. *Geography Compass*, *4*(11), 1648–1663. https://doi.org/10.1111/j.1749-8198.2010.00400.x

Tague, C. L., & Grant, G. E. (2004). A geological framework for interpreting the low-flow regimes of Cascade streams, Willamette River basin, Oregon. *Water Resources Research*, *40*, W04303. https://doi.org/10.1029/2003WR002629

Tague, C. L., & Grant, G. E. (2009). Groundwater dynamics mediate low-flow response to global warming in snow-dominated alpine regions. *Water Resources Research*, *45*, W07421. https://doi.org/10.1029/2008WR007179

Tague, C. L., Grant, G. E., Farrell, M., Choate, J., & Jefferson, A. (2008). Deep groundwater mediates streamflow response to climate warming in the Oregon Cascades. *Climatic Change*, *86*(1–2), 189–210. https://doi.org/10.1007/s10584-007-9294-8

Tallaksen, L. M. (1995). A review of baseflow recession analysis. *Journal of Hydrology*, *165*(1-4), 349–370. https://doi.org/10.1016/0022-1694(94)02540-R

Tan, X., & Gan, T. Y. (2015). Contribution of human and climate change impacts to changes in streamflow of Canada. *Scientific Reports*, *5*(1), 17,767. https://doi.org/10.1038/srep17767

Tennant, C. J., Crosby, B. T., Godsey, S. E., VanKirk, R. W., & Derryberry, D. R. (2015). A simple framework for assessing the sensitivity of mountain watersheds to warming-driven snowpack loss. *Geophysical Research Letters*, *42*, 2814–2822. https://doi.org/10.1002/2015GL063413

Tsai, Y. (2017). The multivariate climatic and anthropogenic elasticity of streamflow in the eastern United States. *Journal of Hydrology: Regional Studies*, *9*, 199–215. https://doi.org/10.1016/j.ejrh.2016.12.078

Van Loon, A. F. (2015). Hydrological drought explained. *Wiley Interdisciplinary Reviews Water*, *2*(4), 359–392. https://doi.org/10.1002/wat2.1085

Vano, J. A., Das, T., & Lettenmaier, D. P. (2012). Hydrologic sensitivities of Colorado River runoff to changes in precipitation and temperature. *Journal of Hydrometeorology*, *13*(3), 932–949. https://doi.org/10.1175/JHM-D-11-069.1

Wolock, D. M. (2003). Flow characteristics at U.S. Geological Survey streamgages in the conterminous United States (USGS Numbered Series No. 2003–146). Retrieved from http://pubs.er.usgs.gov/publication/ofr03146

Wolock, D. M., & McCabe, G. J. (1999). Explaining spatial variability in mean annual runoff in the conterminous United States. *Climate Research*, *11*(2), 149–159. https://doi.org/10.3354/cr011149

Ye, S., Li, H.-Y., Huang, M., Ali, M., Leng, G., Leung, L. R., et al. (2014). Regionalization of subsurface stormflow parameters of hydrologic models: Derivation from regional analysis of streamflow recession curves. *Journal of Hydrology*, *519*, 670–682. https://doi.org/10.1016/j.jhydrol.2014.07.017

Erratum

In the originally published version of this article, Table S1, which is a table listing data published in the article, was missing from the supporting information. The file has since been added and this version may be considered the authoritative version of record.